Hindawi
Shock and Vibration
Volume 2021, Article ID 6637909, 13 pages
https://doi.org/10.1155/2021/6637909

Research Article

Seismic Damage Prediction Method for Lining Structures Based on the SEDR Principle

Q. Zheng,[1] C. L. Xin,[2,3] Y. S. Shen,[1,4] Z. M. Huang,[3] and B. Gao[1,4]

[1]*Key Laboratory of Transportation Tunnel Engineering, Ministry of Education, School of Civil Engineering, Southwest Jiaotong University, Chengdu, Sichuan, China*
[2]*State Key Laboratory of Geohazard Prevention and Geoenvironment Protection, Chengdu University of Technology, Chengdu, Sichuan, China*
[3]*College of Environment and Civil Engineering, Chengdu University of Technology, Chengdu, Sichuan, China*
[4]*National Engineering Laboratory for Technology of Geological Disaster Prevention in Land Transportation, Southwest Jiaotong University, Chengdu, Sichuan, China*

Correspondence should be addressed to C. L. Xin; xinchunlei@cdut.edu.cn

Received 3 October 2020; Revised 20 December 2020; Accepted 24 December 2020; Published 7 January 2021

Academic Editor: Giuseppe Ruta

The safety and stability of lining structures are core concerns of tunnel and underground engineering. It is crucial to determine whether a lining structure would crack and which direction the crack would expand with seismic excitation. In previous literature, the principle based on stress and strain has been widely used to predict the seismic damage of lining structures, whereas it cannot specify the cracking modes. Taking account of that deficiency, this paper introduces the strain energy density ratio (SEDR) principle and proposes a seismic damage prediction method for lining structures, which can precisely predict the crack positions and expansion directions. Moreover, numerical simulations of the typical seismic damage sections of two tunnels in the Great Wenchuan Earthquake and a calculating example of the theoretical equations are conducted to verify the proposed method. In summary, the numerical simulation results show that the arch springing cracks first, and the invert cracks next; then the cracks expand to the spandrel, and finally, they form oblique cracks, annular cracks, and longitudinal cracks, whose positions and patterns are in accordance with the field investigation results. In terms of the calculating example results, the obtained two-fold SEDR and cracking angle θ are 1.87 and −6.28°, respectively, which are consistent with the numerical simulation results. Therefore, one can see that the proposed seismic damage prediction method based on the SEDR principle is quite accurate. This method can be used to predict the seismic damage of lining structures and provide a reference for the research of the damage mechanism of tunnels.

1. Introduction

As an important part of lifeline engineering, tunnel and underground engineering faces challenges in avoiding high-intensity seismic zones due to line requirements. Therefore, a tunnel may be severely damaged and difficult to repair if the tunnel is struck by a strong earthquake, even leading to extreme property losses and casualties. It is crucial to address the issue of potential lining structure cracking and to investigate which direction those cracks expand with seismic excitation. This is of great significance to the evaluation of tunnel safety and the aseismic design of tunnels.

The research on the seismic damage of lining structures primarily focuses on three aspects. The first aspect is the collection, analysis, and inversion of seismic damage data. Much work has been done in this aspect to research the damage mechanism of tunnels [1–4]. The second aspect is the experimental researches on tunnel models. For instance, large shaking table model tests [5–9] were conducted, which have obtained fruitful achievements in the field of seismic affecting factors of lining structures. The third aspect is seeking breakthroughs in theoretical analyses, which focuses on establishing constitutive models to obtain the stress state of lining structures with seismic excitation [10–12]. In view

of the existing research methods of the damage mechanism of tunnel structures, experimental analyses and numerical simulations all use the principle based on stress and strain [13–15]. In terms of the application of this principle in the damage prediction, yielding implies damage, whereas the crack positions and expansion directions are not specified [16–19].

Originally, the cracking modes of materials were predicted by the normal stress ratio principle, whereas it was limited in unidirectional composite materials [20]. Afterwards, the strain energy density ratio (SEDR) principle was proposed, extending the range of damage prediction to fibre composite materials [21]. With deep exploration of the SEDR principle, the range of its application was extended to all the orthotropic materials [22]. In the last decade, the SEDR principle has been widely applied in brittle materials (e.g., rock materials and concrete materials) to research the prediction methods of the crack position [23–27], crack expansion [28–32], and fatigue damage [33–35].

Aiming to analyse the seismic response of tunnel structures, this paper introduces the initial damage variable of concrete materials and conducts numerical simulations based on the SEDR principle to simulate the typical seismically damaged sections of two highway tunnels in the Great Wenchuan Earthquake. Furthermore, combining with the Mohr–Coulomb slip principle, the crack positions and expansion directions of lining structures can be predicted by analysing the strain energy density ratios of the lining elements. In addition, this paper compares the numerical simulation results with the field investigation results and conducts a calculating example, indicating that the proposed seismic damage prediction method for lining structures based on the SEDR principle can precisely and accurately predict the crack positions and expansion directions, which can provide a reference for the research on the damage mechanism of tunnels.

2. SEDR Principle

The SEDR of an element is calculated from the stress ratio and strain ratio of the calculating element, which is specifically described as follows.

The element stress ratio is the ratio of the stress in a certain direction and the critical stress in that direction, which can be expressed as

$$\begin{cases} \sigma_{ij}' = \dfrac{\sigma_{ij}}{\sigma_{ijc}}, \\ \\ \tau_\theta' = \dfrac{\tau_\theta}{\tau_{\theta c}}, \end{cases} \tag{1}$$

where σ_{ij} is the normal stress in the ij direction, σ_{ijc} is the critical stress in the ij direction, τ_θ is the shear stress of the plane at angle θ, $\tau_{\theta c}$ is the shear stress of the cracking plane (shown in Figure 1(a)), and i or $j = 1$, 2, and 3 represent the directions of the X-axis, Y-axis, and Z-axis, respectively.

The element strain ratio is the ratio of the strain in a certain direction and the critical strain in that direction, which can be expressed as

$$\begin{cases} \varepsilon_{ij}' = \dfrac{\varepsilon_{ij}}{\varepsilon_{ijc}}, \\ \\ \gamma_\theta' = \dfrac{\gamma_\theta}{\gamma_{\theta c}}, \end{cases} \tag{2}$$

where ε_{ij} is the normal strain in the ij direction, ε_{ijc} is the critical strain in the ij direction, γ_θ is the shear strain of the plane at angle θ, and $\gamma_{\theta c}$ is the shear strain of the cracking plane.

The ε_{ijc} and $\gamma_{\theta c}$ can be obtained by

$$\begin{cases} \varepsilon_{ijc} = \dfrac{\sigma_{ijc}}{E_{ij}}, \\ \\ \gamma_{\theta c} = \dfrac{\tau_{\theta c}}{G_\theta}, \end{cases} \tag{3}$$

where E_{ij} is the elastic modulus in the ij direction and G_θ is the shear modulus of the plane at angle θ.

Accordingly, the strain energy density S_R can be expressed as

$$S_R = \frac{1}{2}\sigma_{ij}'\varepsilon_{ij}'. \tag{4}$$

Considering the orthotropic mechanical properties of the concrete materials of lining structures, they have different elastic moduli and shear moduli in different directions. Similarly, considering the initial damage of concrete materials, the initial damage coefficient D_i is introduced. Therefore, the elastic modulus and shear modulus of concrete can be expressed as

$$\begin{cases} E_i = D_i \times E_0, \\ \\ G_i = D_i \times G_0 = \dfrac{D_i E_0}{2(1+\upsilon)}, \end{cases} \tag{5}$$

where E_0 is the initial elastic modulus and G_0 is the initial shear modulus.

Assuming that Poisson's ratio is not affected by the initial damage, (4) can be transformed into

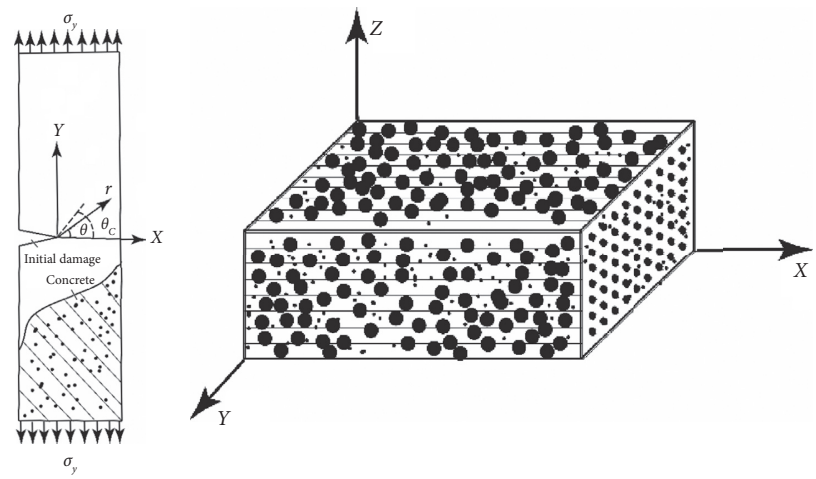

Figure 1: Tensile damage and coordinate system of concrete materials: (a) tensile damage; (b) coordinate system.

$$S_R = \begin{cases} \frac{1}{2}\left[\left(\frac{\sigma_1}{\sigma_{1c}}\right)^2 + \left(\frac{\sigma_2}{\sigma_{2c}}\right)^2 - \frac{\gamma_{12}}{D_1 E_{11}}\sigma_1\sigma_2\left(\frac{D_1 E_{11}}{\sigma_{1c}^2} + \frac{D_2 E_{22}}{\sigma_{2c}^2}\right) + \left(\frac{\tau_{12}}{\tau_{12c}}\right)^2\right], \\ \left(\frac{\sigma_2}{\sigma_{2c}}\right)^2 + \left(\frac{\tau_{23}}{\tau_{23c}}\right)^2, \\ \frac{1}{2}\left[\left(\frac{\sigma_1}{\sigma_{1c}}\right)^2 + \left(\frac{\sigma_3}{\sigma_{3c}}\right)^2 - \frac{\gamma_{13}}{D_1 E_{13}}\sigma_1\sigma_2\left(\frac{D_1 E_{11}}{\sigma_{1c}^2} + \frac{D_2 E_{33}}{\sigma_{3c}^2}\right) + \left(\frac{\tau_{13}}{\tau_{13c}}\right)^2\right], \end{cases} \tag{6}$$

where subscripts 1, 2, and 3 represent the directions of the X-axis, Y-axis, and Z-axis, respectively, as shown in Figure 1 (e.g., σ_{11} is the principle stress in X direction and τ_{23} is the shear stress in YZ plane).

The cracking criterion for the SEDR principle is that the two-fold SEDR of the element is greater than or equal to 1, which can be expressed as

$$2S_R \geq 1. \tag{7}$$

Then the crack expands along the θ direction, which minimizes the S_R. Thus, the expansion direction can be determined by

$$\frac{\partial S_R}{\partial \theta} = 0, \frac{\partial^2 S_R}{\partial \theta^2} > 0, \quad \text{when } \theta = \theta_c. \tag{8}$$

If there are multiple minima through a material element, the crack will expand along the θ_c direction, which makes S_R the largest of the minima. Thus, the expansion direction can be determined by

$$\frac{\partial S_R}{\partial \theta} = 0,$$
$$\theta = \theta_c, \tag{9}$$
$$S_R = (S_R)_{\min}^{\max}.$$

Structures composed of concrete materials usually have large size. From the microscopic view, concrete materials are not homogeneous mediums. However, from the macroscopic view, stones, sand, cement, and other materials are distributed uniformly and nondirectionally in the concrete space. Therefore, the concrete materials can be divided into many uniformly distributed elements, and then the SEDR principle can be applied in the concrete materials. Transforming the space problem into three plane problems, considering that the concrete materials have same mechanical properties along the Y-axis and Z-axis, and only taking the uniaxial tensile damage of concrete into account, equation (10) can be obtained as

$$\begin{cases} \sigma_{1c} = \sigma_1 \cos\theta^2 + \sigma_2 \sin\theta^2 + 2\tau_{12} \sin\theta\cos\theta, \\ \sigma_{2c} = \sigma_1 \sin\theta^2 + \sigma_2 \cos\theta^2 - 2\tau_{12} \sin\theta\cos\theta, \\ \tau_{12c} = (\sigma_2 - \sigma_1)\sin\theta\cos\theta + \tau_{12}^2(\cos\theta^2 - \sin\theta^2). \end{cases} \tag{10}$$

Substituting (10) into (6), the expansion direction can be determined by (8) and (9). In particular, when the material is isotropic and other affecting factors are not taken into account, $\sigma_{ic} = \sigma_0$, $\tau_{\theta c} = \tau_0$, $E_i = E_0$, and $G_\theta = G_0$ are all constants, and then (6) can be simplified to

$$\begin{aligned} S_R &= \frac{1}{2}\left(\sigma_i'\varepsilon_i' + \tau_\theta'\gamma_\theta'\right) = \frac{1}{2}\left[\left[\frac{\sigma}{\sigma_0}\right]^2 + \left[\frac{\tau}{\tau_0}\right]^2\right], \\ &= \frac{1}{2}\left[\left[\frac{\sigma_0 \sin^2\theta}{\sigma_0}\right]^2 + \left[\frac{\sigma_0 \sin\theta_T.\cos\theta}{\tau_0}\right]^2\right]. \end{aligned} \tag{11}$$

When S_R reaches the maximum value, (12) can be obtained as

$$\sin^2\theta\left[1 - \left[\frac{\tau_0}{\sigma_0}\right]^2\right] = \frac{1}{2}. \tag{12}$$

Making $\alpha = (\tau_0/\sigma_0)$, then the expansion direction can be expressed as

$$\theta = \arcsin\sqrt{\frac{1}{2\left(1-\alpha^2\right)}}. \tag{13}$$

3. Numerical Simulation Based on the SEDR Principle

Based on seismic damage investigation data and design data of tunnels of national trunk way line 318 in the Great Wenchuan Earthquake on 12th May, 2008, two typical structural sections, K24 + 380 − K24 + 460 of the Shaohuoping tunnel and K13 + 520 − K13 + 550 of the right line of the Zipingpu tunnel, were selected for the numerical simulation. Using discrete element method, the numerical simulation is based on the Mohr–Coulomb slip principle and the SEDR principle [36]. Herein, the Mohr–Coulomb slip principle is used to obtain the principal stresses and shear stresses of the elements, whereas the SEDR principle is used to predict whether the element cracks or not. In consideration of the design data, the size of Shaohuoping tunnel model (shown in Figure 2) was taken as $X \times Y \times Z = \text{length} \times \text{width} \times \text{height} = 80.0\text{ m} \times 60.0\text{ m} \times 80.0\text{ m}$, whereas the length of Zipingpu tunnel model was taken as 30 m. The inner outline of the tunnel is shown in Figure 3. Besides, the material of lining structures adopted C30 concrete material with a thickness of 30 cm, and the buried depth of the Shaohuoping tunnel was 43.5 m, whereas the Zipingpu tunnel had a buried depth of 110 m. The model was established after static balancing, and the displacement field was cleared after rebalancing. Furthermore, a free field was applied around the boundary of the model (shown in Figure 3), a viscoelastic boundary was applied at the bottom of the model, and an intercepted 25 s Wolong EW component seismic wave was input (shown in Figure 4). In regard to the geological conditions, the surrounding rock of the Shaohuoping tunnel simulation section was grey-white block granodiorite, which was level IV and had 1~2 sets of joints. Meanwhile, the surrounding rock of the Zipingpu tunnel simulation section was sandstone intercalated with thin layers of mudstone, which was level III and level V. The corresponding mechanical parameters of the materials and joints of the model are listed in Table 1 and Table 2, which are obtained referring to the design data of two tunnels. According to the past experimental results [37] (the axial tensile strength of the vertical moulding specimens is 1.82 MPa, and the axial tensile strength of the horizontal moulding specimens is 3.22 MPa), the transverse tensile strength and transverse shear strength are taken as half of the longitudinal tensile strength and longitudinal shear strength, respectively, and the mechanical parameters of the concrete lining in different directions are listed in Table 3.

The stresses and strains of the discretized lining elements (the size of the element was controlled by the maximum length of side, which was 1 m) were monitored (shown in Figures 5–7). According to the monitoring data, the damage of lining elements was predicted by both the program based on Mohr–Coulomb slip principle and the self-compiled program based on the SEDR principle. The block was predicted to be cracking when the monitoring data of the element satisfied the SEDR principle and shear slip occurred at the interface of the minimum SEDR, and the crack was predicted to expand along the Mohr–Coulomb slip plane. If the monitoring data of the lining element did not satisfy the SEDR principle and Mohr–Coulomb slip principle, then the prediction moved on to the next moment. The prediction process is shown in Figure 8.

The SEDR principle was used to predict the cracking of the Shaohuoping tunnel simulation section in whole dynamic time history, and the crack patterns and expansion directions at different times were obtained (shown in Figure 9). During the excitation of the Wolong EW component seismic wave, the arch springing of the Shaohuoping tunnel simulation section cracked first, and the invert cracked next. When the seismic wave was loaded to 14 s, some cracks at arch springing expanded to the spandrel and formed annular cracks, other cracks expanded obliquely and formed longitudinal cracks, and it is worth noting that the cracks appeared both inside and outside of the tunnel and had the signs of penetration. In addition, there were cracks and faults at the construction joint.

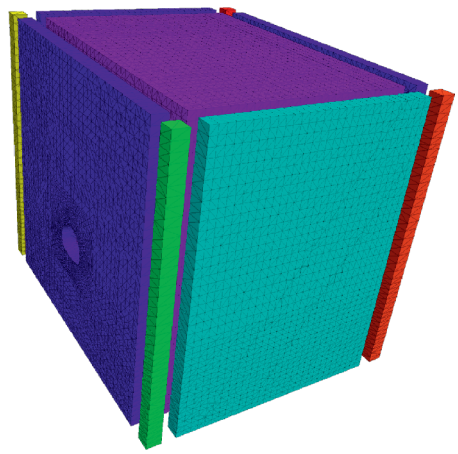

Figure 2: Typical outline of the tunnel.

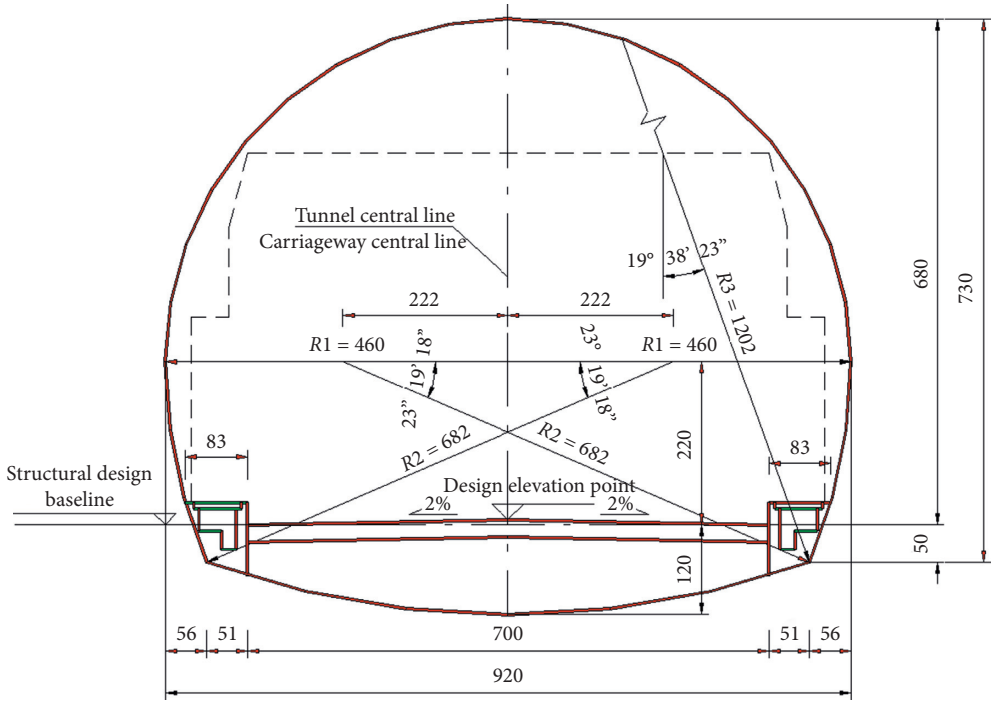

Figure 3: Axonometric drawing of the model with free field boundary.

Subsequently, comparisons of the crack diagrams of the field investigation results and the crack diagrams of the numerical simulation results are shown in Figures 10 and 11. The comparisons show that the crack positions and expansion directions are identical, which are also consistent with the field investigation photos shown in Figure 12. Therefore, it can be concluded that the proposed seismic damage prediction method for lining structures based on the SEDR principle is applicable to the predict the seismic damage of lining structures, and the cracking modes predicted by the SEDR principle are absolutely accurate.

4. Calculating Example

Considering the longitudinal and transverse mechanical differences of concrete materials, the corresponding mechanical parameters of the concrete lining are as listed in Table 3 and the adopted calculation model is shown in Figure 3. Besides, the no. 1985 element (shown in Figure 13) at 3.52 s of the calculation of the Shaohuoping tunnel is taken for calculation, and the calculated maximum principal stress and shear stress at 3.52 s are shown in Figure 13. Furthermore, the following values can be obtained according

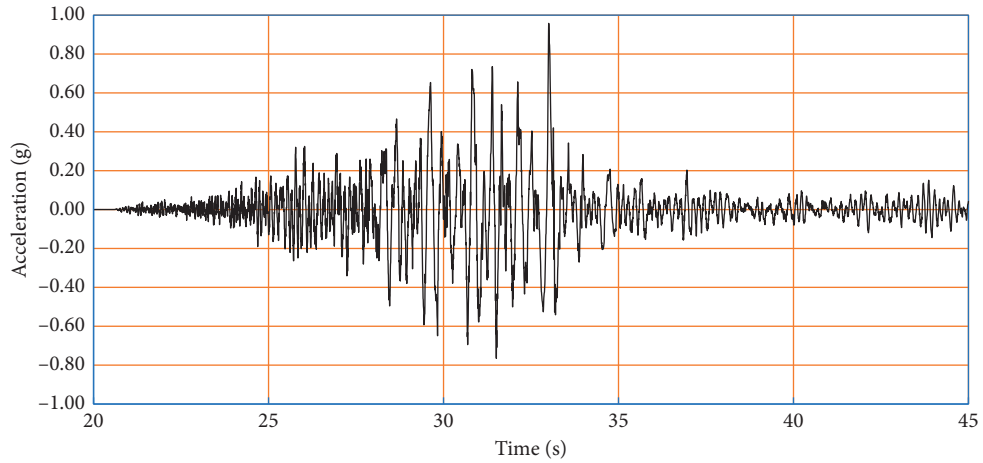

Figure 4: Acceleration time history of the Wolong EW component seismic wave in the Great Wenchuan Earthquake.

Table 1: The mechanical parameters of materials.

Material	Elastic modulus (MPa)	Poisson's ratio	Density (kg·m^{-3})	Angle of internal friction (°)	Cohesion(MPa)
C30 concrete material	30000	0.3	2500	45	5
Level III surrounding rock	10000	0.3	2300	40	1
Level V surrounding rock	6000	0.35	2000	25	0.1
Level IV surrounding rock	12000	0.3	2200	35	0.05

Table 2: The mechanical parameters of joints.

Joint	Normal stiffness (GPa·m^{-1})	Shear stiffness (GPa·m^{-1})	Cohesion (MPa)	Angle of friction (°)	Tensile strength (MPa)
Joint set 1	4.5	0.68	0.027	26	0
Joint set 2	6	1.2	0.045	28	0
Interface of lining blocks	10	4	0.4	40	2
Interface of other blocks	1	0.62	0.01	20	0.002

Table 3: The mechanical parameters of the concrete lining in different directions.

Direction	Tensile strength (MPa)	Compressive strength (MPa)	Shear strength (MPa)	Elastic modulus (MPa)	Shear modulus (MPa)	Initial damage coefficient
Longitudinal	1.43	14.3	2.1	30000	11500	0.95
Transverse	0.71	14.3	1.1	30000	11500	0.95

to the monitoring data: $\sigma_{11} = 1.57$MPa, which is a tensile stress; $\sigma_{33} = -0.269$MPa, which is a compressive stress; and $\tau_{12} = \tau_{13} = 0.9$MPa. Substituting the above values and the values listed in Table 3 into (6) yields that the value of the two-fold SEDR of this element is 1.87, which is greater than 1, expressed as (14). Thus, the SEDR of this element is in

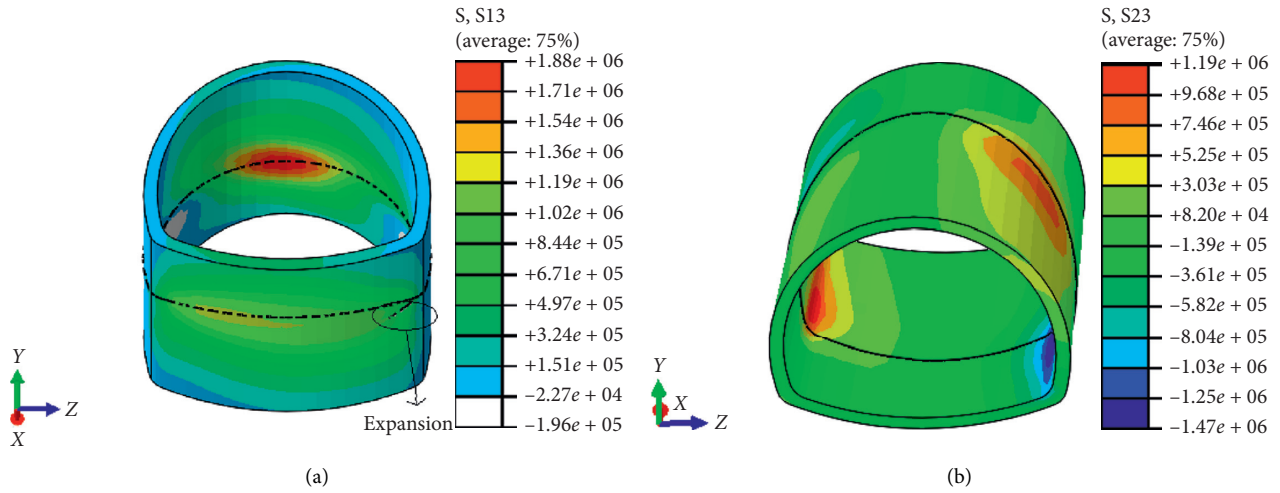

Figure 5: Shear stress monitoring and cracking prediction (local): (a) bottom view; (b) top view.

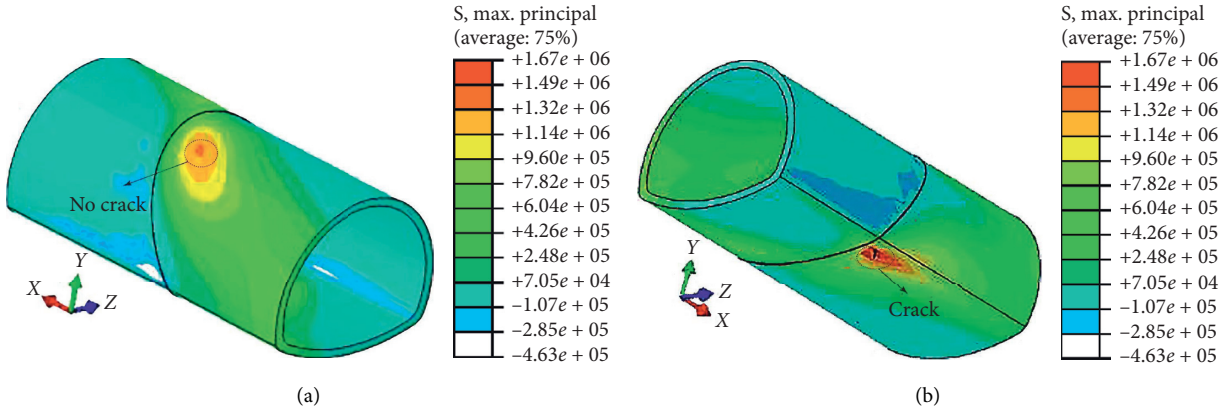

Figure 6: Principal stress monitoring and cracking prediction (local): (a) top view; (b) bottom view.

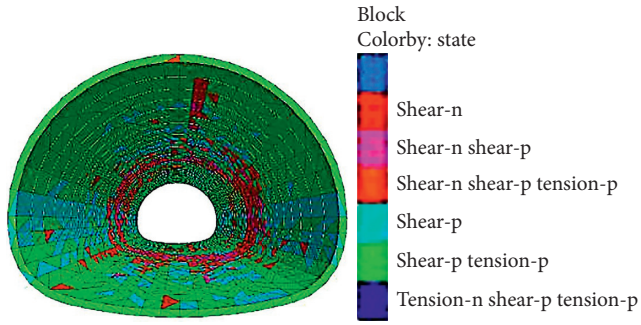

Figure 7: Contrast of the plastic zone in discretized lining model.

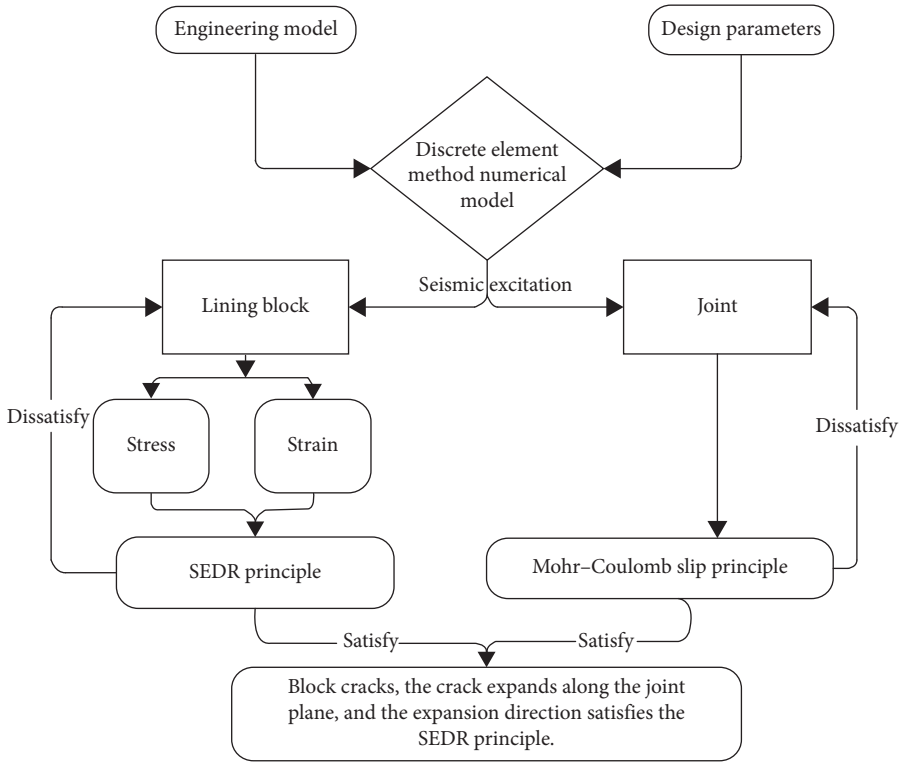

Figure 8: Prediction process of the numerical simulation based on the SEDR principle and the Mohr–Coulomb slip principle.

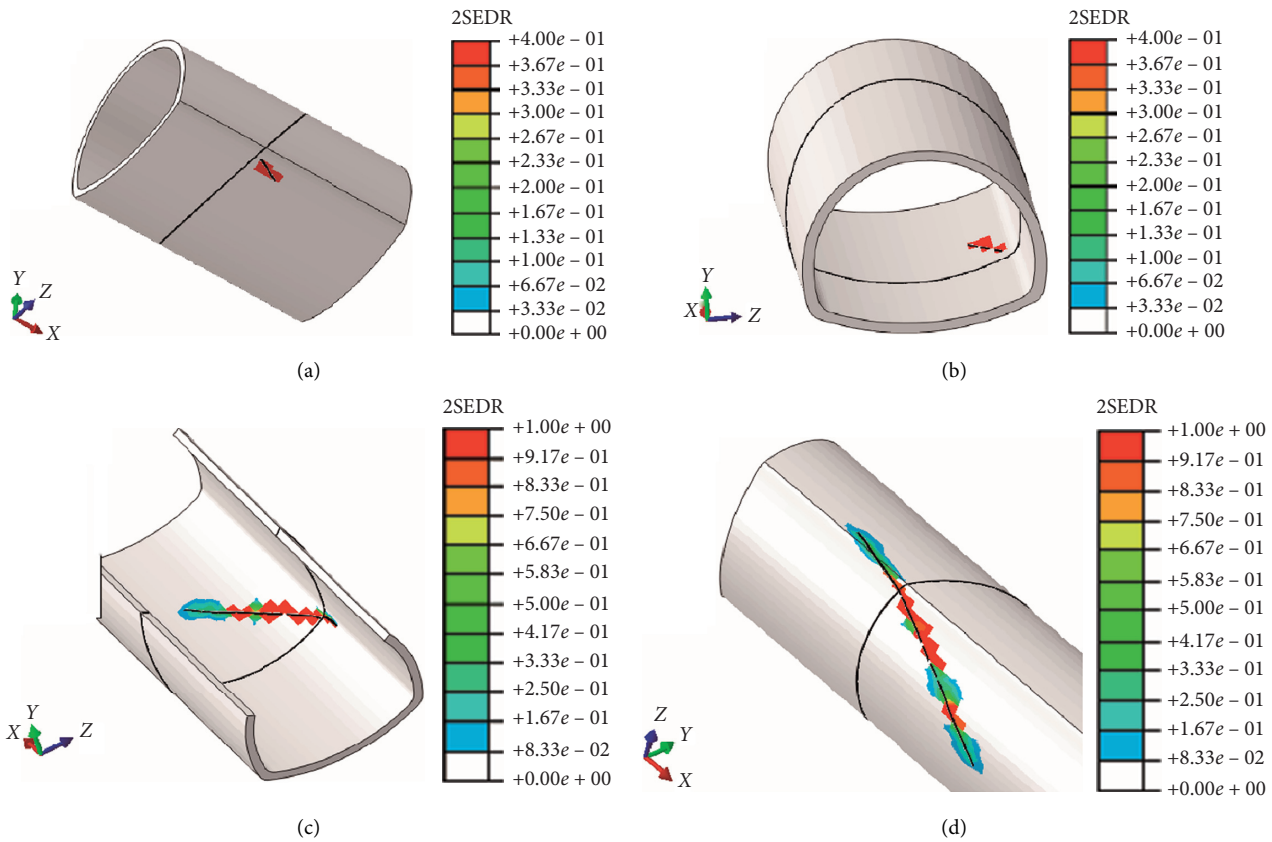

Figure 9: Continued.

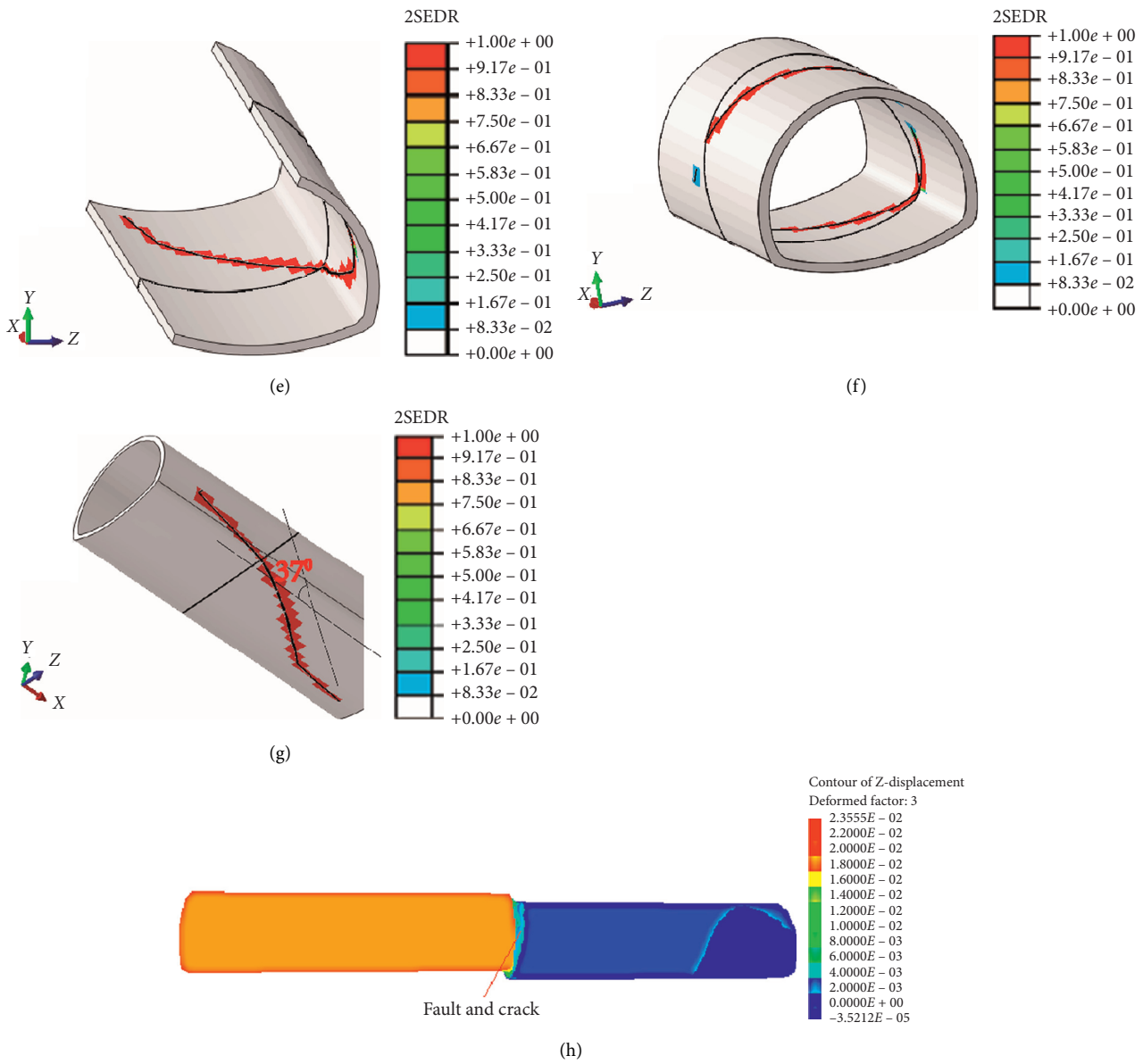

Figure 9: Cracking prediction of the Shaohuoping tunnel with the SEDR principle: (a) the initial crack outside the arch springing at 3.52 s; (b) the crack inside the invert at 6 s; (c) the crack expansion inside the invert at 10 s; (d) the crack expansion outside the arch springing at 14 s; (e) the crack expansion inside the invert at 17 s; (f) the annular expansion at 22 s; (g) the crack expansion outside the arch springing at 25 s; (h) the fault and crack at the construction joint.

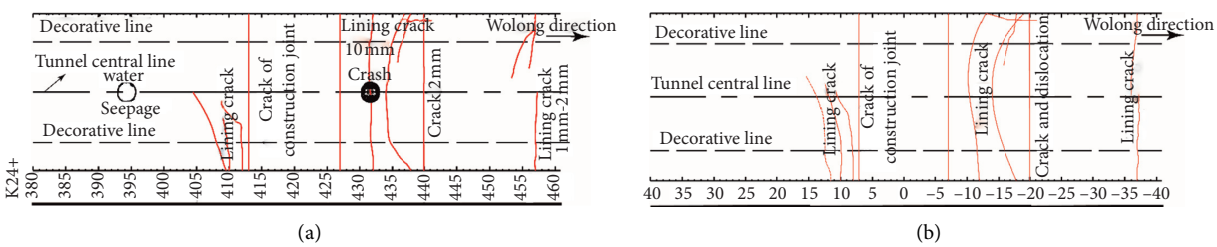

Figure 10: Seismic damage of the Shaohuoping tunnel simulation section: (a) field investigation results; (b) numerical simulation results.

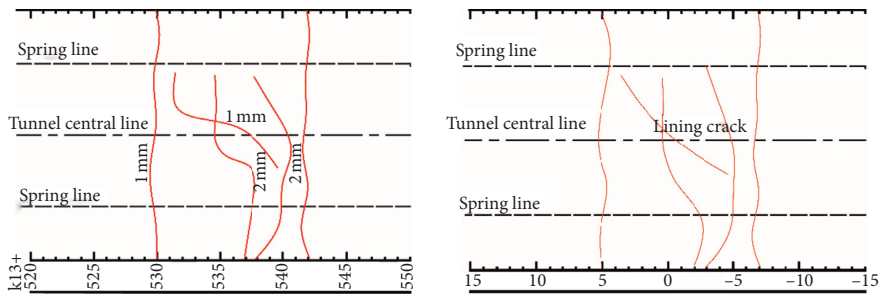

FIGURE 11: Seismic damage of the simulation section of the Zipingpu tunnel right line: (a) field investigation results; (b) numerical simulation results.

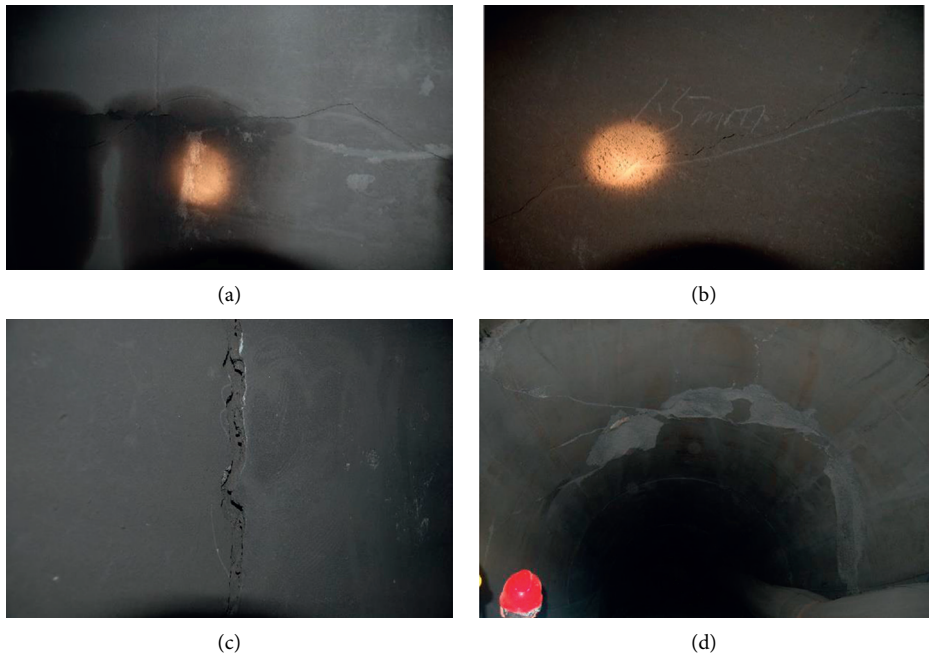

FIGURE 12: Seismic damage investigation photos in the Great Wenchuan Earthquake: (a) oblique crack; (b) longitudinal crack; (c) annular crack; (d) crack and fault.

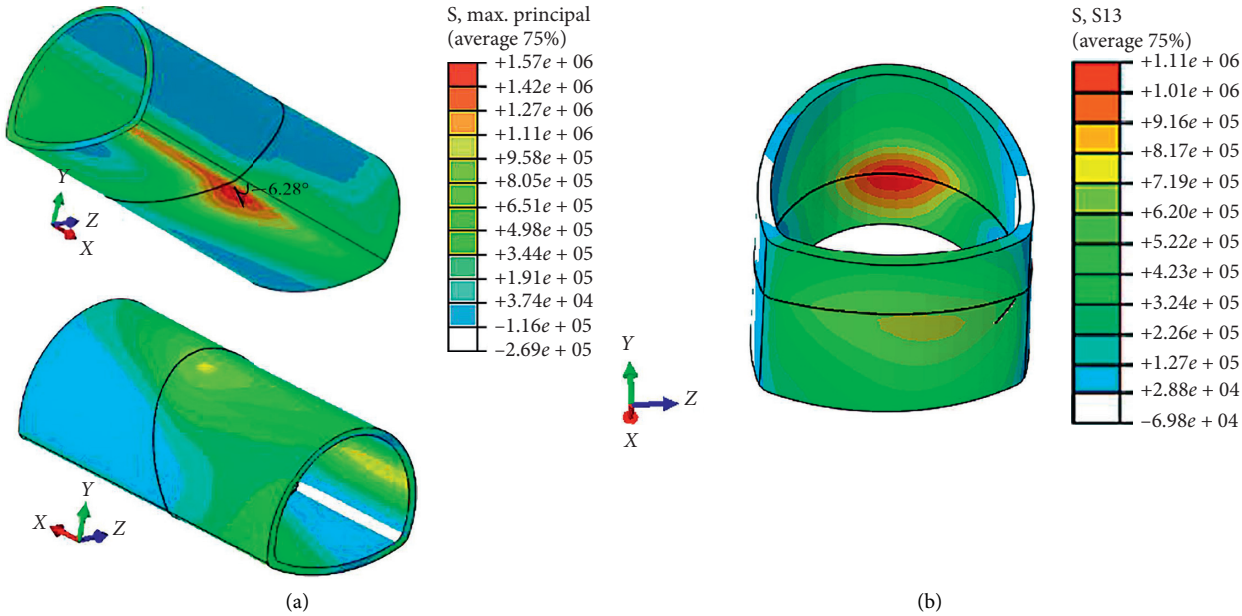

FIGURE 13: Stress monitoring of the Shaohuoping tunnel (3.52 s): (a) maximum principal stress; (b) shear stress.

accordance with the cracking criterion of the SEDR principle.

$$\begin{aligned} 2S_R &= \left(\frac{\sigma_1}{\sigma_{1c}}\right)^2 + \left(\frac{\sigma_3}{\sigma_{2c}}\right)^2 - \frac{\gamma_{12}}{D_1E_{11}}\sigma_1\sigma_3\left(\frac{D_1E_{11}}{\sigma_{1c}^2} + \frac{D_3E_{33}}{\sigma_{3c}^2}\right) + \left(\frac{\tau_{13}}{\tau_{13c}}\right)^2, \\ &= \left(\frac{1.57}{1.43}\right)^2 + \left(\frac{0.269}{14.3}\right)^2 - \frac{0.9/30000}{0.9\times 30000}1.57\times 0.269\left(\frac{0.9\times 30000}{1.43^2} + \frac{0.9\times 30000}{14.3^2}\right) + \left(\frac{0.9}{1.1}\right)^2. \\ &= 1.87 > 1. \end{aligned} \tag{14}$$

Substituting monitoring values into (10), the cracking angle can be calculated as (15). Furthermore, (16) can be obtained by simplifying (15), solving the absolute value of cracking angle as 6.28°, which can be expressed as (17). In addition, according to the calculating results, σ_1 is a positive tension and σ_2 is a negative pressure; hence the cracking angle θ is −6.28°.

$$\begin{aligned} 1.43 &= 1.57\cos\theta^2 - 0.269\sin\theta^2 + 2\times 0.9\sin\theta\cos\theta, \\ 1.839\sin\theta^2 &- 1.8\sin\theta\cos\theta = 0.14, \end{aligned} \tag{15}$$

$$\begin{aligned} \sin(2\theta+\varphi) &= 0.848, \\ \tan\varphi &= \left(\frac{1.839}{1.8}\right), \end{aligned} \tag{16}$$

$$\theta = 0.108\text{rad} = 6.28^0. \tag{17}$$

5. Conclusions

This paper proposes a seismic damage prediction method for lining structures based on the SEDR principle, which can predict the crack positions and expansion directions. Subsequently, the numerical simulation of typical seismic damage sections of the Shaohuoping and Zipingpu tunnels in the Great Wenchuan Earthquake based on the SEDR principle is conducted to verify this method. Moreover, a calculating example is conducted to validate the accuracy and precision of the proposed method. Herein, the conclusions are summarized as follows:

(1) The numerical simulation results show that the arch springing cracks first, and the invert cracks next; then the cracks expand to the spandrel, and finally, they form oblique cracks, annular cracks, and longitudinal cracks, whose positions and patterns are in accordance with the field investigation results.

(2) In the calculating example, the two-fold SEDR and cracking angle θ of no. 1985 element are calculated to be 1.87 and −6.28°, respectively, which are consistent with the numerical simulation results.

(3) The proposed method based on the SEDR principle is applicable to predict the seismic damage of lining structures, and the crack positions and expansion directions can be precisely predicted by this method.

Data Availability

The data in Figure 4 used to support the findings of this study are included within the article.

Conflicts of Interest

The authors declare that they have no conflicts of interest.

Acknowledgments

This research was supported by the Miaozi Engineering Key Project from Science and Technology Department of Sichuan Province (Grant no. 2020JDRC0078), the State Key Laboratory of Geohazard Prevention and Geoenvironment Protection (China) Open Fund (Grant no. SKLGP2020K018), and the National Natural Science Foundation of China (Grants nos. 51678501 and 51778540).

References

[1] X. Li and L. Weng, "Numerical investigation on fracturing behaviors of deep-buried opening under dynamic disturbance," *Tunnelling and Underground Space Technology*, vol. 54, pp. 61–72, 2016.

[2] M. Tao, H. Zhao, X. Li, and K. Du, "Failure characteristics and stress distribution of pre-stressed rock specimen with circular cavity subjected to dynamic loading," *Tunnelling and Underground Space Technology*, vol. 81, pp. 1–15, 2018.

[3] Z. Z. Li, Y. J. Jiang, and C. A. Zhu, "Seismic energy response and damage evolution of tunnel lining structures," *European Journal of Environmental and Civil Engineering*, vol. 23, no. 6, pp. 758–770, 2019.

[4] C. L. Xin, Z. Z. Wang, and J. Yu, "The evaluation on shock absorption performance of buffer layer around the cross section of tunnel lining," *Soil Dynamics and Earthquake Engineering*, vol. 131, Article ID 106032, 2020.

[5] C. L. Xin, Z. Z. Wang, and B. Gao, "Shaking table tests on seismic response and damage mode of tunnel linings in diverse tunnel-void interaction states," *Tunnelling and Underground Space Technology*, vol. 77, pp. 295–304, 2018.

[6] C. L. Xin, Z. Z. Wang, J. M. Zhou, and B. Gao, "Shaking table tests on seismic behavior of polypropylene fiber reinforced

concrete tunnel lining," *Tunnelling and Underground Space Technology*, vol. 88, pp. 1–15, 2019.

[7] Z. Z. Wang, L. Jiang, and Y. Gao, "Shaking table test of seismic response of immersed tunnels under effect of water," *Soil Dynamics and Earthquake Engineering*, vol. 116, pp. 436–445, 2019.

[8] G. Yan, B. Gao, Y. Shen, Q. Zheng, and K. Fan, "Shaking table test on seismic performances of newly designed joints for mountain tunnels crossing faults," *Advances in Structural Engineering*, vol. 23, no. 2, pp. 248–262, 2019.

[9] Y. S. Huang, Z. Z. Wang, J. Yu, X. Zhang, and B. Gao, "Shaking table test on flexible joints of mountain tunnels passing through normal fault," *Tunnelling and Underground Space Technology*, vol. 98, Article ID 103299, 2020.

[10] M. K. Darabi, R. K. Al-Rub, and E. A. Masad, "Constitutive modeling of fatigue damage response of asphalt concrete materials with consideration of micro-damage healing," *International Journal of Solids and Structures*, vol. 50, no. 19, pp. 2901–2913, 2013.

[11] C. Little, J. Fortin, and Y. Guéguen, "Brittle creep and subcritical crack propagation in glass submitted to triaxial conditions," *Journal of Geophysical Research: Solid Earth*, vol. 120, no. 2, pp. 879–893, 2015.

[12] C. Bouyer, H. Dumontet, and F. Voldoire, "Dissipative homogenised reinforced concrete (DHRC) constitutive model dedicated to reinforced concrete plates under seismic loading," *International Journal of Solids and Structures*, vol. 73-74, pp. 78–98, 2015.

[13] M.-D. Wei, F. Dai, N.-W. Xu, and T. Zhao, "Fracture prediction of rocks under mode I and mode II loading using the generalized maximum tangential strain criterion," *Engineering Fracture Mechanics*, vol. 186, pp. 21–38, 2017.

[14] M. M. Liu, A. Razmi, and F. Berto, "Tangential strain-based criteria for mixed-mode I/II fracture toughness of cement concrete," *Fatigue & Fracture of Engineering Materials & Structures*, vol. 41, no. 1, pp. 129–137, 2018.

[15] M. Nain, M. M. Abdulazeez, and M. A. ElGawady, "Behavior of high strength concrete: filled hybrid large—small rupture strains FRP tubes," *Engineering Structures*, vol. 209, Article ID 110264, 2020.

[16] Y. Liu, F. Dai, P. Fan, and L. Dong, "Experimental investigation of the influence of joint geometric configurations on the mechanical properties of intermittent jointed rock models under cyclic uniaxial compression," *Rock Mechanics and Rock Engineering*, vol. 50, no. 6, pp. 1453–1471, 2017.

[17] X. F. Xu, H. B. Li, Q. B. Zhang, and J. Zhao, "Dynamic fragmentation of rock material: characteristic size, fragment distribution and pulverization law," *Engineering Fracture Mechanics*, vol. 199, pp. 739–759, 2018.

[18] G. Jiang, A. Rinaldi, and I. Iturrioz, "The fracture process in quasi-brittle materials simulated using a lattice dynamical model," *Fatigue & Fracture of Engineering Materials & Structures*, vol. 42, no. 12, pp. 2709–2724, 2019.

[19] Z. Lyu, J. Rivière, and Q. Yang, "On the mechanics of granular shear: the effect of normal stress and layer thickness on stick-slip properties," *Tectonophysics*, vol. 763, pp. 86–99, 2019.

[20] M. A. Marone and C. T. Herakovich, "Predicting crack growth direction in unidirectional composites," *Journal of Composite Materials*, vol. 20, no. 1, pp. 67–85, 1986.

[21] L. W. Tsai and S. Y. Zhang, "Prediction of mixed-mode cracking direction in random, short-fibre composite materials," *Composites Science and Technology*, vol. 31, no. 2, pp. 97–110, 1988.

[22] S. Y. Zhang and L. W. Tsai, "Extending tsai-hill and norris criteria to predict cracking direction in orthotropic materials," *International Journal of Fracture*, vol. 40, no. 4, pp. R101–R104, 1989.

[23] H. P. Lee and J. E. Olson, "The effect of remote and internal crack stresses on mixed-mode brittle fracture propagation of open cracks under compressive loading," *International Journal of Fracture*, vol. 207, no. 2, pp. 229–242, 2017.

[24] X. P. Zhou and H. Q. Yang, "Dynamic damage localization in crack-weakened rock mass: strain energy density factor approach," *Theoretical and Applied Fracture Mechanics*, vol. 97, pp. 289–302, 2018.

[25] Y. D. Shou, X. P. Zhou, and Q. H. Qian, "A critical condition of the zonal disintegration in deep rock masses: strain energy density approach," *Theoretical and Applied Fracture Mechanics*, vol. 97, pp. 322–332, 2018.

[26] S. M. J. Razavi, M. R. M. Aliha, and F. Berto, "Application of an average strain energy density criterion to obtain the mixed mode fracture load of granite rock tested with the cracked asymmetric four-point bend specimens," *Theoretical and Applied Fracture Mechanics*, vol. 97, pp. 419–425, 2018.

[27] F. Gong, J. Yan, and X. Li, "A peak-strength strain energy storage index for rock burst proneness of rock materials," *International Journal of Rock Mechanics and Mining Sciences*, vol. 117, pp. 76–89, 2019.

[28] R. Luo, L. Marsavina, H. Filipescu, and T. Voiconi, "Assessment of brittle fracture for PUR materials using local strain energy density and theory of critical distances," *Theoretical And Applied Fracture Mechanics*, vol. 79, pp. 62–69, 2015.

[29] Y. Căplescu, Y. Ju, F. Li, and H. Sun, "The fractal characteristics and energy mechanism of crack propagation in tight reservoir sandstone subjected to triaxial stresses," *Journal of Natural Gas Science And Engineering*, vol. 32, pp. 415–422, 2016.

[30] F. Gao, M. R. Ayatollahi, and T. Borsato, "Local strain energy density to predict size-dependent brittle fracture of cracked specimens under mixed mode loading," *Theoretical and Applied Fracture Mechanics*, vol. 86, pp. 217–224, 2016.

[31] F.-Q. Ferro, S. Luo, and J.-Y. Yan, "Energy storage and dissipation evolution process and characteristics of marble in three tension-type failure tests," *Rock Mechanics and Rock Engineering*, vol. 51, no. 11, pp. 3613–3624, 2018.

[32] J. Justo, J. Castro, and S. Cicero, "Energy-based approach for fracture assessment of several rocks containing u-shaped notches through the application of the SED criterion," *International Journal of Rock Mechanics and Mining Sciences*, vol. 110, pp. 306–315, 2018.

[33] M. R. M. Aliha, F. Berto, and A. Mousavi, "On the applicability of ASED criterion for predicting mixed mode I + II fracture toughness results of a rock material," *Theoretical and Applied Fracture Mechanics*, vol. 92, pp. 198–204, 2017.

[34] M. R. Razavi, M. R. Ayatollahi, and F. Berto, "Rock fracture toughness under mode II loading: a theoretical model based on local strain energy density," *Rock Mechanics and Rock Engineering*, vol. 51, no. 1, pp. 243–253, 2018.

[35] D. Radaj, "State-of-the-art review on the local strain energy density concept and its relation to the j-integral and peak stress method," *Fatigue & Fracture of Engineering Materials & Structures*, vol. 38, no. 1, pp. 2–28, 2015.

[36] J. Hamdi, L. Scholtès, and M. Souley, "Effect of discretization at laboratory and large scales during discrete element modelling of brittle failure," *International Journal of Rock Mechanics and Mining Sciences*, vol. 100, pp. 48–61, 2017.

[37] J. E. Al Heib and M. Mellas, "Application of backscattered electron imaging to concrete materials," *Cement and Concrete Research*, vol. 23, no. 3, pp. 576–580, 1993.